Preprint
UCRL-JC-139232-PT-1-REV-1

Uranyl-Fluoride (^{233}U) Solutions in Spherical Stainless Steel Vessels with Reflectors of Be, Ch_2 and Be-Ch_2 Composites

D. Heinrichs

This article was submitted to
International Criticality Safety Benchmark Evaluation Project
Working Group Meeting, Jackson Hole, WY, June 11-15, 2001

U.S. Department of Energy

Lawrence
Livermore
National
Laboratory

April 24, 2001

Status and Future of Microwave Cavity Axion Searches

Karl van Bibber and Darin Kinion
Lawrence Livermore National Laboratory, Livermore, CA 94550

We review the status of an ongoing large-scale search for axions which may constitute the dark matter of our Milky Way halo. The experiment is based on the microwave cavity technique proposed by Sikivie, and marks a 'second-generation' to the original experiments performed by the Rochester-Brookhaven-Fermilab collaboration, and the University of Florida group. Sensitivity to galactic axions has been achieved, at least for one important model coupling. A remarkable breakthrough in making near-quantum limited dc SQUID amplifiers in the several hundred megahertz range has provided the enabling technology for a major upgrade of this effort. By improving the noise temperature by more than an order of magnitude, a much more sensitive search may be carried out, greatly improving the prospects for discovering the axion.

1 Introduction and Historical Perspective

After more than twenty years, the Peccei-Quinn mechanism still remains the most natural and minimal extension of the Standard Model to enforce strong-CP symmetry.[1] The resulting axion[2] has likewise defied either being discovered or excluded, although the allowed mass for the axion is now bounded within a three decade range or so, $10^{-6} - 10^{-3}$ eV. The lower bound results from cosmology (axions overclose the Universe),[3] and the upper bound from astrophysics (axions quench the neutrino signal from SN1987a).[4] Scenarios evading these limits are of course possible,[5] but strained.

Nevertheless, finishing the job on the axion will not be easy work. Within the original axion model it was presumed that the symmetry-breaking scale was the electroweak scale, $f_a \sim 250$ GeV, implying axions of mass $\sim$100 keV, and with couplings strong enough to ensure their detection in accelerator- and reactor-based experiments. These axions were quickly ruled out, and new models were created for which the symmetry-breaking scale could be arbitrarily high.[6,7] As both the mass and all couplings of the axion are inversely proportional to the symmetry-breaking scale (1,2), removing the axion to very large values of f_a implied that axions would be both extremely light and possess couplings so weak as to render them 'invisible'. In Eqn. 2 we exhibit the axion's coupling to two photons, specifically relevant to this experiment; the parameter E/N can be any rational number.

$$m_a[eV] \approx 0.6\ eV \frac{10^7\ GeV}{f_a\ [GeV]} \tag{1}$$

$$g_{a\gamma\gamma} = \frac{\alpha_e}{\pi f_a}\left(\frac{E}{N} - \frac{2(4+z)}{3(1+z)}\right) \tag{2}$$

where $z \equiv m_u/m_d \sim 0.5$ is the ratio of the up- and down-quark masses and α_e is the electromagnetic fine structure constant.

Interestingly, however as the axion mass becomes lighter, the mass density of the Universe in axions created during the Big Bang increases: [8]

$$\Omega_a \equiv \frac{\rho_a}{\rho_c} \approx \left(\frac{0.7\times 10^{-5} eV}{m_a}\right)^{\frac{7}{6}} \left(\frac{200 MeV}{\Lambda_{QCD}}\right)^{\frac{3}{4}} \left(\frac{70 km/s Mpc}{H_o}\right)^2 \tag{3}$$

where ρ_c is the critical density of the universe, Λ_{QCD} is the QCD scale, and H_o is the Hubble constant. As axions would have been produced as a zero-temperature Bose gas, and would have never been in thermal equilibrium with anything else, it was clear that a very light axion would be an attractive Cold Dark Matter candidate, possibly the predominant component of the mass of the Universe. How to detect it was another matter.

In 1983, Pierre Sikivie solved the conundrum of how to detect dark matter axions with vanishingly small couplings.[9] This technique relies on the Primakoff effect, *i.e.* the two-photon interaction of a pseudoscalar, where one of the photons is virtual. Here, dark matter axions would convert into a weak microwave signal in a strong magnetic field - a sea of virtual photons - the process being resonantly enhanced by a high-Q cavity resonator. The signal corresponds to the total energy of the axion, mass plus kinetic, and being non-relativistic, the fully thermalized signal is expected to be nearly monochromatic, $\Delta E_a/m_a \sim \beta^2 \sim 10^{-6}$. In addition to the virial component, the axion signal may additionally possess fine structure in the form of a spectrum of extremely narrow peaks ($\Delta E_a/m_a \sim 10^{-18}$) due to late-infall axions. Should the axion exist, this fine structure - Doppler-modulated in frequency with both the earth's motion about its own axis and around the sun - would contain a wealth of information about the history of our galactic formation.

While the microwave cavity technique made the axion detectable in principle, the expected signal would still be extraordinarily weak: [9,10]

$$P_a \approx 10^{-21} W \left(\frac{B_0}{7.7T}\right)^2 \left(\frac{V}{200l}\right)\left(\frac{C}{0.65}\right)\left(\frac{Q}{90000}\right)\left(\frac{\nu}{0.7\ GHz}\right)\left(\frac{\rho_a}{\rho_{halo}}\right) \tag{4}$$

where B_0 is the background magnetic field, V is the cavity volume, C is a mode-dependent form factor, Q is the loaded quality factor, ν is the resonant

frequency, and ρ_a is the local halo axion density. For the parameters of this experiment and assuming that $\rho_a = \rho_{halo} \approx 450$ MeV/cc,[11] the power from KSVZ axions is typically $5 \times 10^{-22} W$.

As one does not know the mass of the axion, the cavity must be tuned in small steps, the resonance condition being $\nu = m_a$. The rate at which the mass region is swept out, either to find the axion at a given s/n or exclude it at a given % confidence level is dictated by the Dicke radiometer equation:

$$\frac{S}{N} = \frac{P_a}{P_N}\sqrt{Bt} = \frac{P_a}{k_B T_s}\sqrt{\frac{t}{B}} \tag{5}$$

where k_B is Boltzmann's constant and B is the bandwidth. For a given SNR, our scanning rate is:

$$\frac{d\nu}{dt} \approx \left(\frac{25 MHz}{month}\right)\left(\frac{4}{SNR}\right)^2\left(\frac{6\ K}{T_s}\right)^2 \tag{6}$$

where $T_s = T_c + T_a$ is the system noise temperature, specifically the sum of the physical temperature of the cavity T_c and the noise temperature of the amplification chain T_a. Equation 5 makes plain that an arbitrarily small signal may be made statistically significant by increasing the signal power ($P_a \propto B^2 V$), decreasing the system noise temperature or by integrating longer. For a practical search covering a mass range expressed in decades, the latter is not an option. Technology and resources also limit one's ambitions regarding the magnet. Therefore the key to the discovery of the axion is the technology of ultra-low noise microwave amplifiers.

One could legitimately wonder if there was not another method to determine the possible existence of the axion, in a broadband way in mass, and independent of the assumption that it constitutes the dark matter. Considerable thought and effort has been devoted to this question over the years, and the conclusion seems firm that no laboratory experiment even remotely approaches the required sensitivity for very light axions.[12] In the end, if the axion is to be discovered, we believe that it will rely on the prodigious density of axions produced by the Big Bang and further aggregated by our galactic gravitational potential. Requiring the axion to constitute the dark matter should not be viewed as an independent strong assumption. Rather, should a light axion exist at all, it could hardly fail to be cosmologically significant.

Two pilot experiments were performed in the late 1980's, one by a Rochester-Brookhaven-Fermilab (RBF) collaboration,[13] and another by a group at the University of Florida (UF).[14] Both experiments utilized small-volume superconducting solenoidal magnets (up to 8 tesla, over a volume of several liters), and heterojunction-based amplifiers in the 4-20 K noise temperature

range. While falling short by two to three orders of magnitude from sensitivity to KSVZ axions, much practical experience was gained on which the present experiment built. Noteworthy in the RBF effort were extensive modeling of the cavity-amplifier system by the RBF group,[15] and the use of a higher-TM mode to extend the frequency range of the search, albeit at the cost of a greatly reduced cavity form-factor. An important contribution of the research by the UF group was the demonstration of power-combining of two independent cavities, as a first step towards multiplexing many small cavities of high frequency while fully utilizing a large magnetic volume.[16] The design and implementation of the present experiment drew heavily on both the personnel and experience of these two searches.

2 Status of the Present Experiment

Figure 1 shows the apparatus, consisting of the magnet and the insert containing the cavity and cryogenic amplifiers.

2.1 The Magnet

The magnet employed in this search is a superconducting NbTi solenoid constructed by Wang NMR Inc.[17] It is a low current (224 A), high inductance (533 H) design to maximize field stability, which serves to minimize eddy current heating of the cavity. The operating field at the center of the coil is usually 7.62 T.

The current is supplied by a power supply through a pair of vapor-cooled current leads constructed from copper foil. Computer stabilization of the power supply provides field stability of 5 ppm.

The magnet is a warm bore design, meaning that it contains internal thermal shielding between the 4.2 K coil and the inner bore. This allows the magnet to remain cold whether the insert is in place or not. The coil has remained at 4.2 K since its arrival in March, 1995, using an average of 60 liters of liquid helium per day.

2.2 The Cavity and Tuning Rods

The microwave cavity is a right-circular cylinder constructed from stainless steel and plated with ultra-high purity, oxygen-free copper. Annealing the cavity after plating increased the copper's conductivity. The inside diameter is 50 cm and the length is 1 m.

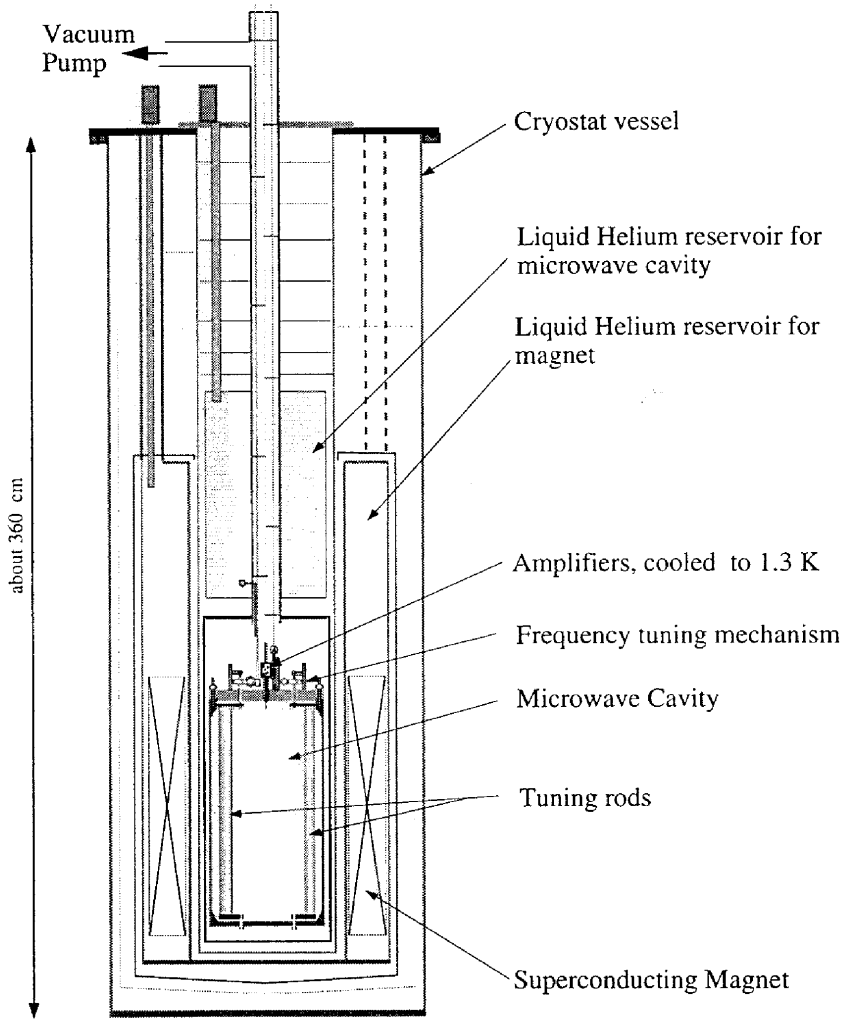

Figure 1: The U.S. Axion search detector.

To maximize the form factor from (4) :

$$C = \frac{1}{B_o^2 V} \frac{\left(\int \bar{E}(x,y,z) \cdot \bar{B}(x,y,z) dV\right)^2}{\int \bar{E}^2(x,y,z) \epsilon(x,y,z) dV} \tag{7}$$

the cavity electric field should be parallel to the static, external magnetic field. The TM_{010} mode has the highest form factor ($C \approx 0.5 - 0.6$), and is therefore used in the search. For this mode, the resonant frequency of the empty cavity is 460 MHz, and the unloaded Q is approximately 200,000.

Moving a combination of metal and dielectric rods, running the full length of the cavity, changes the resonant frequency. These rods can move from the center of the cavity to the wall. The single cavity accommodates two rods.

To achieve the required 500 Hz resolution in resonant frequency it is necessary to move the tuning rods in very fine steps. Stepper motors with a resolution of 1.8°/step followed by a gear reduction of 42000:1 control the rods. The final step size is approximately 80 nm.

2.3 Insert Cryogenics

Superfluid ^{4}He maintains the physical temperature of the cavity near 1.5 K. A capillary tube supplies helium from the 170 liter inner reservoir to a small pool in the bottom of the vacuum can. A valve in the capillary tube regulates the liquid level. A roots blower pumps on the helium, evaporatively cooling the cavity and cryogenic amplifiers to 1.5 K. The pressure of the helium gas in the cavity is roughly 0.1 Torr.

2.4 Cryogenic Amplifiers and Cavity Coupling

The cryogenic amplifiers used in this search are double-balanced GaAs HFET amplifiers supplied by NRAO.[18] The *in situ* measured noise temperatures range from 1.7 - 4.5 K. For minimum noise temperature, it is important that the amplifiers be positioned so that the B field is parallel to the plane of the HFET channels.[18] Cascading two of these amplifiers achieves sufficient gain (35 dB) to render downstream noise contributions negligible.

The amplifiers are capacitively coupled to the cavity using a short length of semi-rigid coax. The linear antenna is formed by removing the outer conductor from the last 5 cm of the coax. The strength of the coupling is varied by changing the insertion depth. Critical coupling is maintained throughout the run, meaning that on resonance the cavity presents a matched load to the first amplifier.

A directional coupler placed between the antenna and the first amplifier allows a direct measurements of the coupling. This coupler is used for measurements of the reflection from the cavity. The first amplifier is effectively critically coupled to the cavity when this reflection is very small on resonance, typically - 30 dB.

A stepper motor similar to the ones used for tuning controls the insertion depth of the antenna. The resolution is approximately 1.5 μm with a 5 cm range of motion.

2.5 Room Temperature Electronics

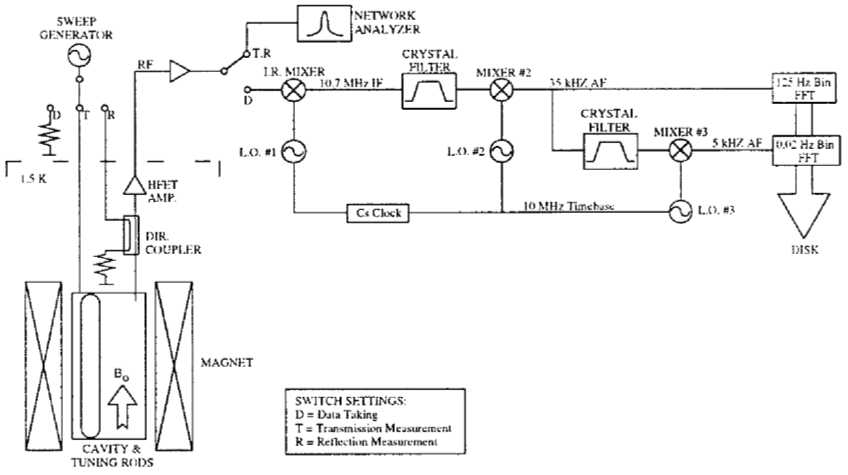

Figure 2: Axion detector schematic.

Figure 2 is a block diagram showing the two major components of the room temperature electronics, the setup for measuring transmission through the cavity and the receiver electronics.

Before data is taken at a given frequency, a transmission measurement is made. For the measurement, power is fed through a second, very weakly coupled port in the cavity and the transmitted power is measured using a scalar network analyzer. A fit of the transmission curve to the sum of a Lorentzian and constant background determines the resonant frequency and Q.

The receiver is simply an extremely sensitive radio receiver with the cavity as the LC tank circuit. First, the 35 dB cryogenic amplification described earlier is followed by 35 dB of room-temperature post-amplification. Next, the signal passes through an image-reject mixer shifting the resonant frequency down to 10.7 MHz. From there, an oven-stabilized, eight-pole crystal filter sets the bandwidth of the measurement at 30 kHz. This filter also prevents image power from entering the subsequent mixing stages. Next, a second mixing stage shifts the center frequency to 35 kHz. This audio signal is then sent to both medium- and high-resolution search channels.

The medium-resolution search channel consists of a Stanford Research Systems [19] FFT spectrum analyzer. The sampling period of the analyzer is 80 msec, giving a frequency resolution of 125 Hz. Each step involves averaging 10000 such spectra, resulting in a 400 point power spectrum with 125 Hz bins. These data are coadded and the result searched for Maxwellian peaks a few bins wide (about 700 Hz) characteristic of thermalized axions in the halo.[20]

An independent, high-resolution search channel operates in parallel to explore the possibility of fine-structure in the axion signal.[21,22] The 35 kHz signal passes through a six-pole crystal filter and third mixing stage to shift the center frequency to 5 kHz. During the 80 seconds that the medium resolution channel is averaging spectra, a PC based DSP takes a single 50 second spectrum and performs an FFT. The resulting frequency resolution is 20 mHz, about the limit imposed by the Doppler shift due to the earth's rotation. These data are searched for coincidences between different scans, as well as coincidences with peaks in the medium resolution data.

2.6 Sensitivity Calibration

The sensitivity of the axion detector is found by measuring the noise power as the physical temperature of the cavity T_c is varied. On resonance, the cavity acts like a 50 Ω termination and emits a noise power $P_c = k_B B T_c$, where B is the bandwidth. The noise power at the output of the amplifier is given by $P = k_B B G(T_c + T_a)$, where G is the gain of the amplifier and T_a is its noise temperature.

The noise temperature of the amplifier T_a is independent of temperature for $T_c < 12$ K, most likely due to inefficient cooling of the HFET channels. The temperature dependence of the gain can be taken out by following the height of a fixed power peak injected into the cavity during the test. The result is a straight-line plot of noise power versus cavity temperature whose intercept gives the noise temperature of the amplifier. Figure 3 gives the result from one of these tests.

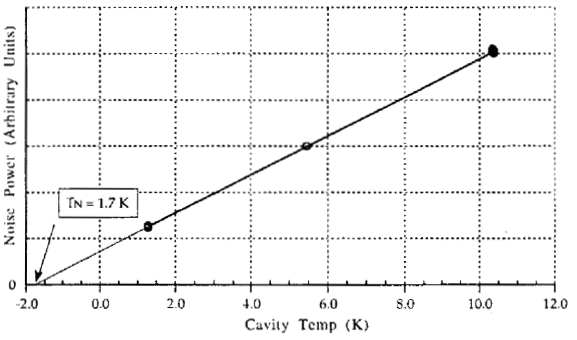

Figure 3: Results from an *in situ* noise temperature test. Several measurements of the noise power were made at three different cavity temperatures.

2.7 Operations

Using LabVIEW [23] software running on a Macintosh computer, this experiment is completely automated. providing 24 hour/day operation. The tasks of the computer include regulating the magnet power supply, controlling the LHe level in the vacuum can, tuning the cavity and tracking the correct mode, maintaining critical coupling, coordinating the two search channels, and logging the data for analysis. In addition, the computer monitors and logs cryogen levels, room and cavity temperatures, magnet coil and lead voltages, pressures, and many other parameters. This system has been very reliable, allowing us to run at well over 90% duty cycle since February 1996.

2.8 Data taking

The first scan performed in a region is sequential, with the cavity frequency stepped in roughly 2 kHz intervals. The computer adjusts the size of the physical steps to maintain the correct frequency shifts. This process is repeated until sufficient integration time is achieved, typically 2-4 times.

This first scan does not always provide uniform coverage, so the software also provides the capability to scan specific regions with differing amounts of integration. This provides a flattened signal-to-noise ratio across the region. Positive fluctuations in this power spectrum are identified as candidate peaks and rescanned. Peaks which are statistical in nature will not reappear and can be eliminated as axion signals.

Candidates which survive the rescan are considered persistent, and must be checked in other ways. Most will disappear when the ports used for reflec-

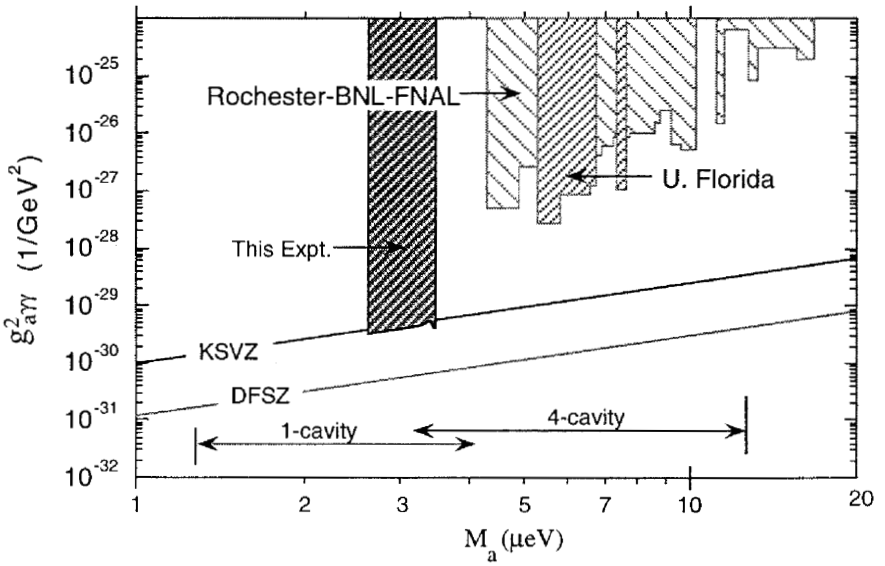

Figure 4: Axion couplings and masses excluded at the 90% confidence level by this experiment as of January 1999. The solid lines indicate the KSVZ and DFSZ model predictions. The arrows at the bottom indicate the coverage of different cavity configurations. Also shown are the results from the two pilot experiments scaled to 90% c.l. and $\rho_a = \rho_{halo}$.

tion and transmission measurements are terminated, signifying that they were external sources leaking into the system. Those few that remained have all been linked to external sources by using an antenna in the room. If a peak were to survive all of these checks, the definitive test would be to see if it appears only when the magnetic field is on.

The only significant complication with this scheme are mode-crossings, regions where the TM_{010} frequency is degenerate with either a TE or TEM mode. When there are two tuning rods in the cavity, often it is possible to move the locations of these crossings and fill in the gaps in the data. When this is not possible, it is necessary to fill the entire cavity with LHe, shifting the frequency of these regions by roughly 3%, before scanning.

So far, no axion signal has been detected. Based on these results, we exclude at 90% confidence a KSVZ axion of mass between 2.5 and 3.3 μeV, assuming that thermalized axions comprise a major fraction of our galactic halo. This exclusion region and the results from two pilot experiments are shown in Figure 4. For more details see Ref. 24.

3 Technology Development

There are two major directions for this experiment to go in the future, up in frequency and down in sensitivity. Higher frequencies will require smaller cavities, which can be power combined to maintain effective use of the magnet volume. Work on this is already underway. Much higher frequencies may be achievable with a lattice of posts inside a larger cavity. Going to lower sensitivity, with the ultimate goal of achieving DFSZ, will require a major upgrade. Two steps in this direction are the development of dc SQUID amplifiers with near quantum-limited noise temperatures and a completely different photon detector employing Rydberg atoms being commissioned in Kyoto.

3.1 Multiple Cavity Arrays

Exploring higher frequency regions will require smaller cavities. However, placing a single, smaller cavity into the magnet would be inefficient. Since the axion signal is coherent over the volume of the cavity ($\lambda_D = h/m_a v \approx 10 - 100m$). it is possible to power combine the signal from multiple cavities and maintain effective use of the magnet volume.

There are several new challenges presented by running with multiple cavities. The most fundamental issue is keeping them all tuned to the same frequency. The mechanical tuning mechanism employed in the single cavity search is not practical when the dimensions of the cavity become small. Instead, work is progressing on new, piezoelectric based tuning and coupling mechanisms, providing equal, if not better step resolution.

A four-cavity array scheduled for commissioning late in 1999 will be the first realization of a multiple cavity array and piezoelectric tuning. With a single alumina tuning rod, this setup will cover the region from 0.81 to 1.1 GHz. Minimum tuning rod motions are on the order of 300 nm, corresponding to a typical frequency resolution of 500 Hz.

3.2 Higher Frequency Cavities

The technique of power-combining signals from many small cavities is only practicle for frequencies up to ≈ 3 GHz. This is because the number of cavities required scales as f_{010}^3, where f_{010} is the frequency of the TM_{010} mode. An alternative for reaching higher frequencies is the strategic placement of metal posts inside a single larger cavity.[16]

Figure 6 shows a triangular lattice of 19 posts inside a circular cavity. With r/R = 0.1, this arrangement raises the TM_{010} frequency by a factor of 5 compared to the empty cavity value. Figure 7 shows the calculated longitudinal

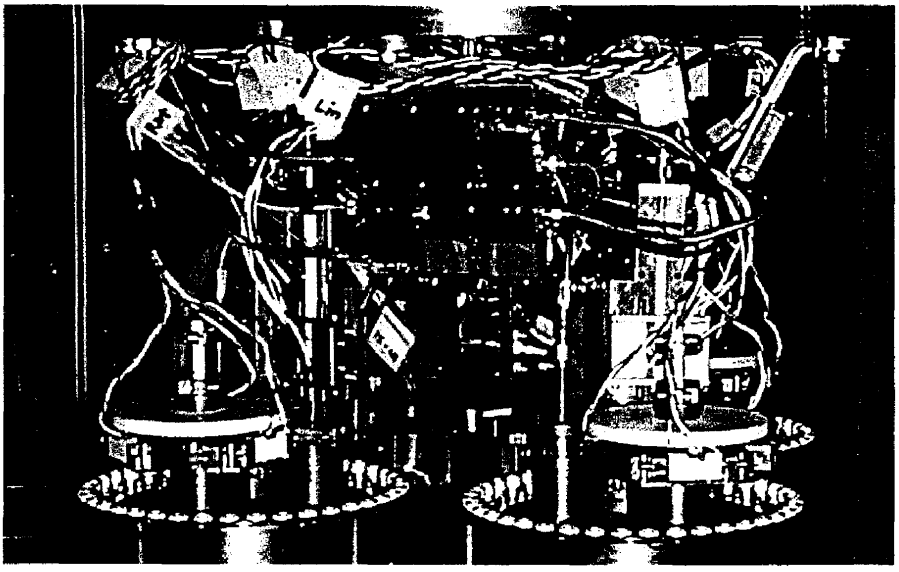

Figure 5: Picture of the four-cavity array.

electric field for this mode. The form factor is ≈ 0.5, a reasonable value for a cavity axion detector. It is important to note that the usable volume in this configuration is 4 times greater than that of the corresponding empty cavity with the same resonant frequency.

Tuning these cavities can not be done with a simple tuning rod as before. Translational symmetry in the axial direction must be maintained to avoid mode-localization, so inserting a small dielectric rod along the axis is also unacceptable. The fundamental frequency scales roughly as a^{-2}, where a is the nearest-neighbor spacing in the lattice, so this must be changed to tune the cavity.

A simple method for changing the lattice spacing is shown in Figure 8. The centered square lattice on the left can be broken down into two square lattices with spacing $2a$. One of the lattices is translated as indicated, and the structure transforms into the rectangular lattice shown on the right. The tuning bandwidth $\Delta f_{010}/f_{010}$ is $\sim 10\%$.

More study is required to determine if this is a feasible method to explore higher frequencies. The biggest concerns are limited tuning bandwidth, constraints on the physical dimensions to avoid mode-localization, possible degradation of the form factor as the cavity is tuned, and the density of inter-

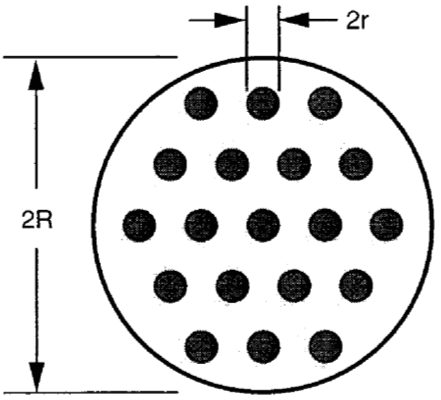

Figure 6: A triangular lattice of 19 posts inside a single circular cavity.

fering TE and TEM modes at higher frequencies. Resolving these issues could extend the mass range of microwave cavity axion searches by another decade.

3.3 DC SQUID Amplifiers

Since the expected power from DFSZ axion conversion is an order of magnitude lower than that from KSVZ axions it would take one hundred times longer to reach similar sensitivity. From Equation 6, the scanning rate goes as T_s^{-2}, therefore, an order of magnitude reduction in system noise temperature would allow a scan at DFSZ sensitivity with the same rate as the present scan with KSVZ sensitivity.

In the present experiment $T_c \approx T_a \approx 1.5$ K, and thus $T_s \geq 3$ K. T_c may be lowered to ~ 200 mK with a dilution refrigerator, but $T_a \geq 1.5$ K for current HFET amplifiers independent of physical temperature below 12 K. In the past two years, however, a group at Berkeley led by John Clarke has developed dc SQUID amplifiers in the 100 - 1000 MHz range specifically for the axion experiment. Noise temperatures as low as 120 mK have been measured at a physical temperature of 500 mK, and unlike HFET amplifiers, the noise temperature in dc SQUID amplifiers is expected to scale with temperature.

The dc SQUID (Figure 9(a)) consists of two Josephson junctions connected in parallel on a superconducting loop. The current-voltage (I-V) characteristics are shown in Fig. 9(b) for $\Phi = n\Phi_0$ and $(n + 1/2)\Phi_0$, where Φ is the flux applied to the loop, n is an integer, and $\Phi_0 = h/2e \approx 2.07 \times 10^{-15}$ Wb is the flux quantum. When the SQUID is biased with a constant current (greater

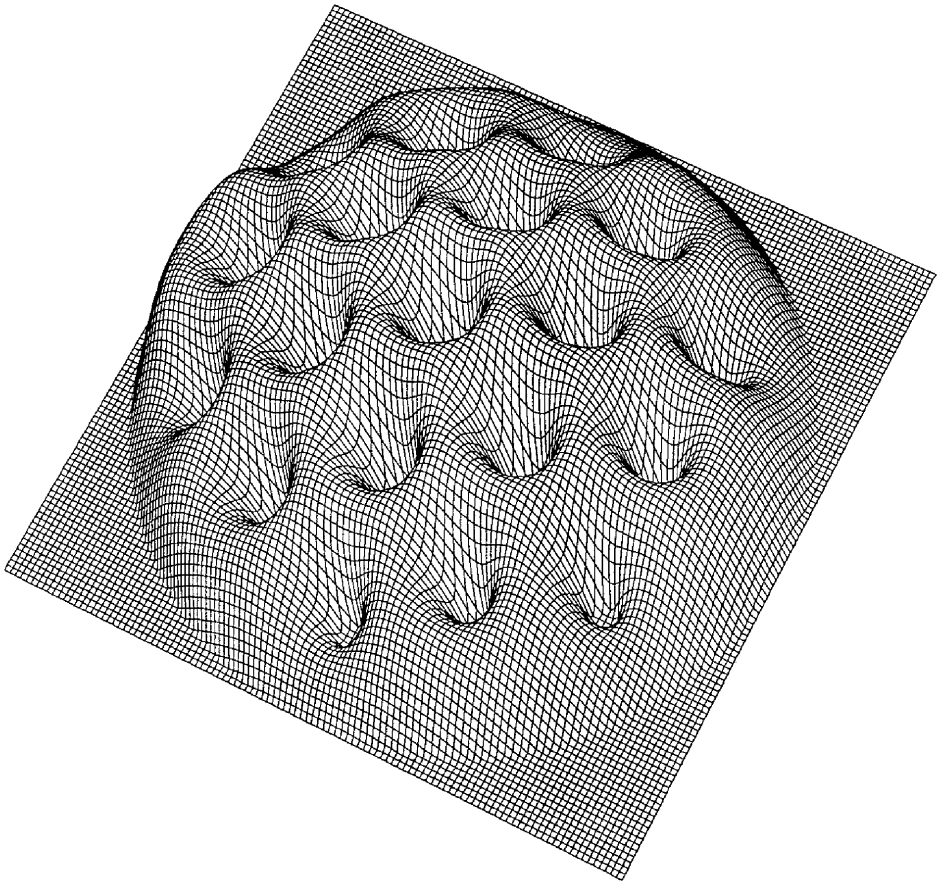

Figure 7: Longitudinal electric field of the TM_{010} mode for the configuration in Figure 6 with r/R = 0.1.

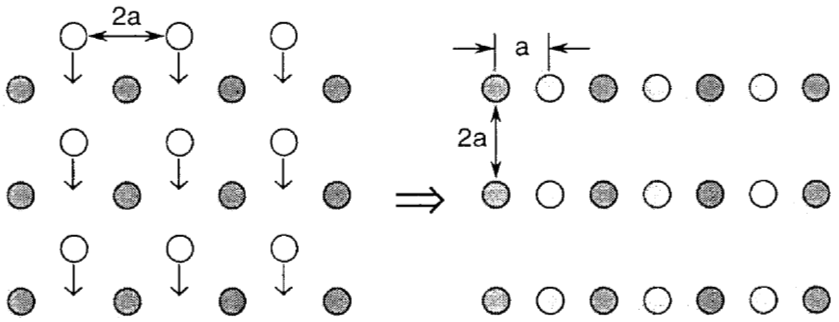

Figure 8: Changing from a centered square lattice to a rectangular lattice.

than $2I_0$ where I_0 is the critical current of each junction), the voltage across the SQUID oscillates with period Φ_0 as Φ is increased (Figure 9(c)). The bias current is adjusted to give the maximum voltage swing, and the SQUID is operated on the steep portion of the $V - \Phi$ curve where the flux-to-voltage transfer coefficient, $V_\Phi \equiv |\partial V/\partial \Phi|_I$, is a maximum. Thus, the SQUID produces an output voltage in response to a small input flux $\delta\Phi(\ll \Phi_0)$, and is effectively a flux-to-voltage transducer. Detailed computer simulations of the signal and noise properties were made by Tesche and Clarke.[25]

The most common configuration of a dc SQUID amplifier is shown in Figure 9(d).[26] The superconducting loop is a square washer with a slit on one side. The loop is closed via a superconducting counter-electrode connected to the washer by two resistively-shunted Josephson junctions. Flux is coupled into the SQUID through a microstrip input coil separated from the washer by a thin insulating layer. Originally, the input signal was coupled between the ends of the coil, forming a simple transformer with the input coil as the primary and SQUID loop as the secondary. This worked for frequencies up to 200 MHz, where the parasitic capacitance between the coil and the SQUID washer becomes too great. Recently, this problem was solved by coupling the input signal between one end of the coil and the SQUID washer, which acts as a ground plane for the coil. A microstrip resonator is thus formed by the open-ended stripline whose impedance is determined by the inductance of the input coil and its ground plane and the capacitance between them. Near the fundamental frequency of the stripline, the gain of the amplifier is strongly enhanced.

The square-washer SQUIDs had inner and outer dimensions of 0.2 mm x

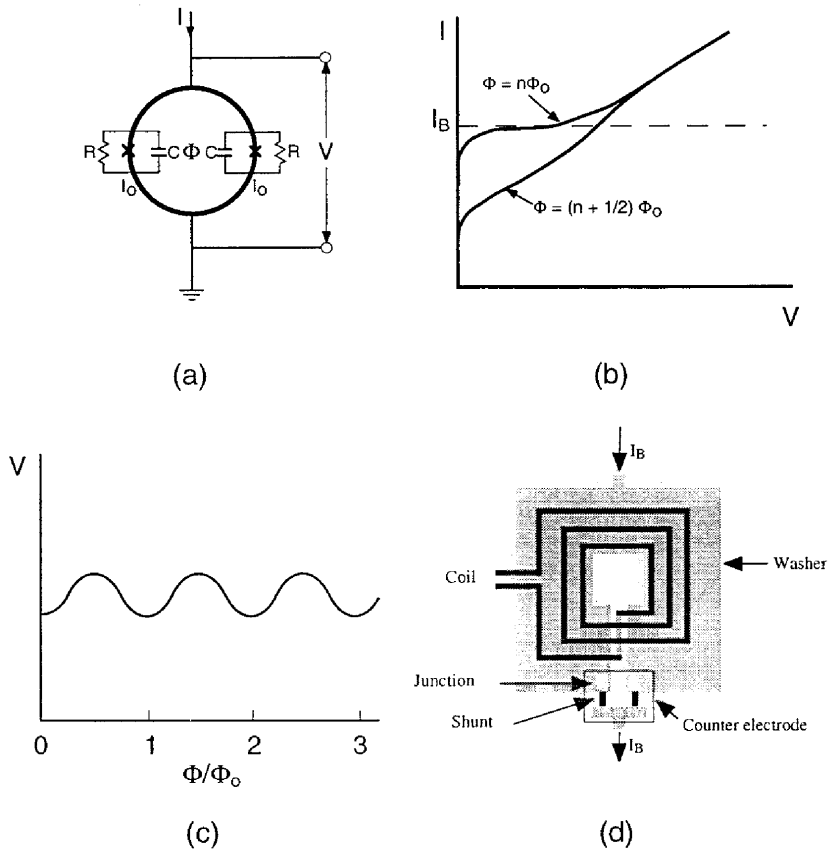

Figure 9: (a) The dc SQUID; (b) I-V characteristics; (c) V vs. Φ/Φ_0 at constant bias current I_B; (d) square washer SQUID.

0.2 mm and 1 mm x 1 mm, and the input coils had a width of 5 μm and lengths ranging from 6 - 71 mm. Figure 10 shows the gain achieved for four different lengths of coil on the same SQUID. The gain is typically 18 dB. Plotting the resonant frequency vs. the length of the microstrip line [Inset, Fig. 10] shows that this frequency goes inversely with the coil length ℓ as expected, provided one adds an additional length of 16 mm to account for the inductance of the input circuitry. By shortening the coil further, the resonant frequency can be moved to a higher value. Figure 11(a) shows the highest frequency achieved

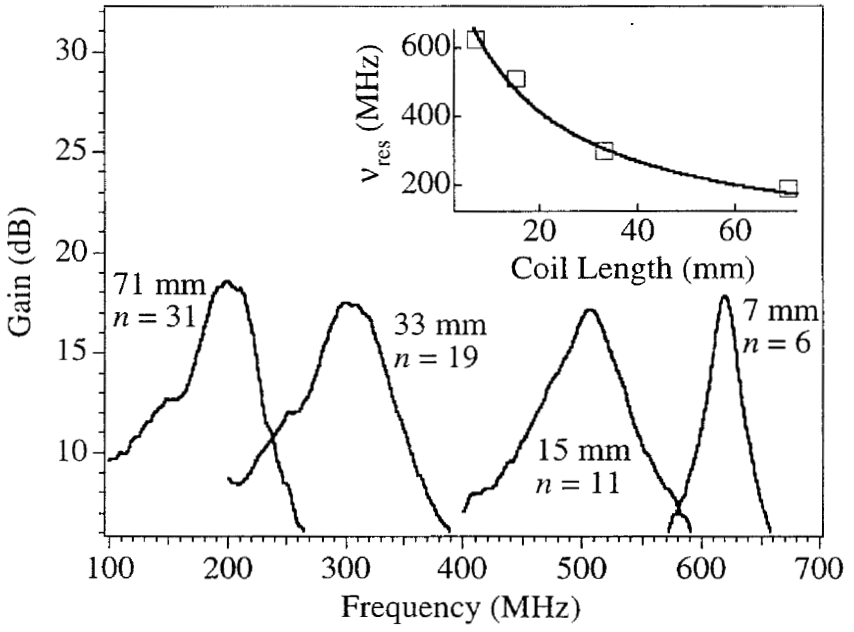

Figure 10: Gain vs. Frequency for four coils of different lengths on the same SQUID. The resonant frequencies vs. length are shown inset; the fitted curve is $(1.49 \times 10^4/(\ell + 16))MHz$, where ℓ is in mm.

to date, 1.06 GHz.

Since dc SQUIDs are inherently very broadband, the bandwidth of these amplifiers is determined by the Q of the input stripline resonator which is typically in the range 2 - 10. Reducing Q would increase the bandwidth, but would sacrifice gain. An alternative is to place a variable reactance at the open end of the stripline which enables one to change the phase shift of the reflected wave and hence change the resonant frequency. In principle, the tuning range is $0.5f_0 - f_0$, where f_0 is the resonant frequency of the open-ended line, as the load is varied from a short to an open.

Tuning of these amplifiers has been accomplished by connecting a pair of GaAs varactor diodes across the previously open end of the microstrip.[27] The capacitance of the diodes is controlled by varying their reverse bias voltage. Figure 11(b) shows the measured gain at 4.2 K, for 9 values of diode capacitance. The resonant frequency is progressively lowered from 195 MHz to 117 MHz as the capacitance is increased; the maximum gain is constant to within

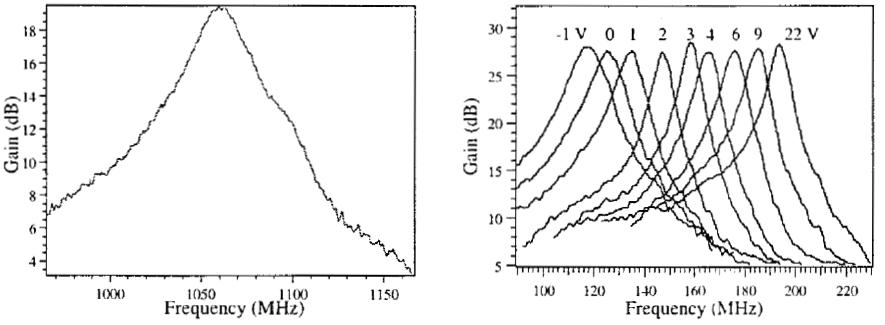

Figure 11: (a) Gain vs. frequency for a 6-turn microstrip SQUID. (b) Gain vs. frequency for a 31-turn SQUID microstrip amplifier at 4.2 K for 9 values of bias voltage applied to the varactor diode.

1 dB. Measurements of the noise temperature at 4.2 K with and without the varactors revealed no discernible difference.

The noise temperature of the SQUID amplifiers was measured using a heated resistor, similar to the method described earlier for the sensitivity calibration. The dominant source of noise in these devices is the Johnson noise from the resistive shunts across the Josephson junctions. This noise scales linearly with temperature, so the noise temperature of dc SQUIDs is expected to be proportional to their physical temperature until either the quantum limit ($T_a = h\nu/k_B \ln 2$)[28] is reached or hot electron effects in the shunts become dominant.

For an early device with an 11-turn input coil at 4.2 K, the gain was 22 dB on resonance, and the noise temperature T_a was 0.9 ± 0.3 K, including an estimated 0.4 K contribution from the room-temperature postamplifier. Subsequently, to reduce this noise contribution, a cooled, single-stage HFET amplifier was used as a postamplifier. Figure 12(a) shows the measured noise temperature, which has a minimum of 0.25 ± 0.1 K at 365 MHz for a bath temperature of 1.8 K. In this measurement, the low-noise bandwidth is limited by the HFET postamplifier and not the SQUID.

In a further attempt to reduce the noise temperature, SQUIDs were cooled to 0.4 - 0.5 K in a charcoal-pumped, single-shot ^{3}He cryostat.[29] The HFET postamplifier was mounted on the 1 K pot. Within the error bars, the noise temperature at each frequency scales with the bath temperature. The system noise temperature at 438 MHz was 0.50 ± 0.07 K, of which 0.38 ± 0.07 K was

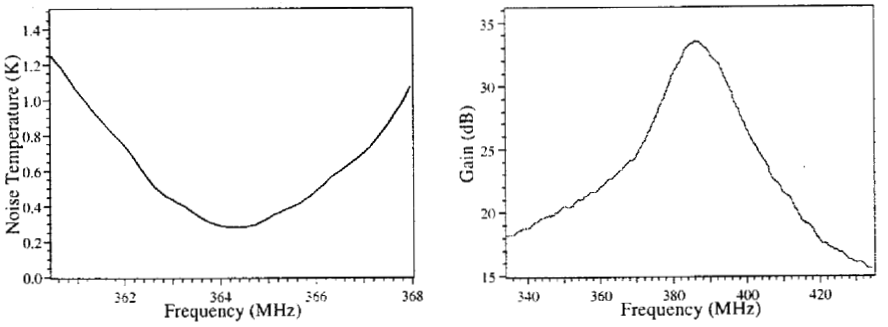

Figure 12: (a) Noise Temperature vs. frequency for a 29-turn microstrip SQUID cooled to 1.8 K, with a HFET amplifier at the same temperature. (b) Measured gain of two cascaded microstrip SQUID amplifiers, with the resonant frequency of the second microstrip tuned with a varactor diode to coincide with that of the first microstrip.

contributed by the postamplifier.

At 500 mK, the noise temperatures are already within a factor of four of the quantum limit, which for a 500 MHz amplifier is approximately 35 mK. Demonstrating a quantum limited amplifier will require a much quieter postamplifier. Toward this end, a second SQUID has been used as a postamplifier to the input SQUID. To prevent the two SQUIDs from interacting, it was necessary to insert an 8 dB attenuator. The resonant frequency of the second SQUID was tuned with a varactor diode to match that of the first SQUID. The maximum power gain at 386 MHz was 33.5 ± 1 dB, as shown in Fig. 12(b).

Since the amplifier must ultimately be connected to a resonant cavity, another test was performed whereby an LC-resonant circuit was inductively coupled to the microstrip SQUID amplifier, with a coupling loss of 2 dB. Figure 13 shows the output of the SQUID at 500 mK vs. frequency, with no applied signal. The peak is due to the Nyquist noise in the resonant circuit, and is consistent with the measured system noise temperature of 500 mK. Because the SQUID can handle a reactive input, no circulator between the cavity and amplifier is required.

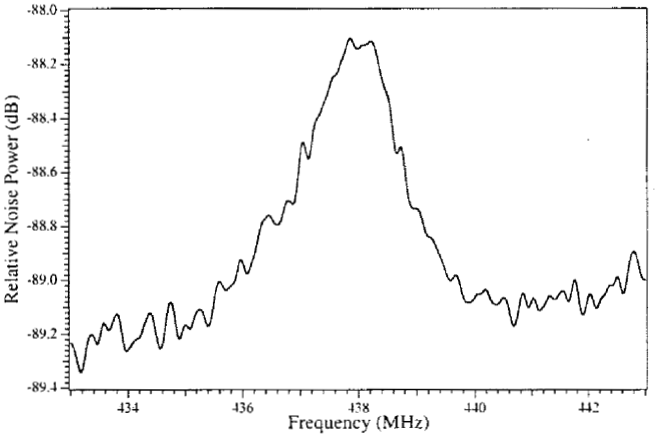

Figure 13: Output noise power of microstrip SQUID at 500 mK with its input coupled to a resonant LC circuit. There was no applied signal.

3.4 Rydberg Atom Single Quantum Detector

Another second-generation axion search is under development at the University of Kyoto. This effort seeks to exploit the extremely low-noise photon counting capability of Rydberg atoms in a Sikivie-type microwave cavity experiment. The initial goal is to sweep out a 10% mass window around $2.4\mu eV$.

Rydberg atoms are atoms (usually alkali metals) where one electron is promoted to a principal quantum number $n \gg 1$, near the ionization limit.[30] The valence electron of such highly excited atoms in hydrogen-like. These Rydberg atom states for $n \sim \mathcal{O}(100)$ are promising as microwave-photon detectors for three reasons: (i) The energy difference between adjacent levels $(E_{n+1} - E_n)$, which scales as n^{-3}, is in the microwave region. For $n \approx 100$ the energy difference is ≈ 7 GHz. (ii) The electric dipole transition rate between adjacent levels, which scales as n^2 is large, implying a high efficiency for absorbing a microwave photon. For $n \approx 100$ the transition rate is 3×10^4/s. (iii) The lifetime of excited states, which scales as n^3 is suitably long. For $n \approx 100$ the lifetime is ≈ 1 ms.

The use of Rydberg atoms for single-quantum counting is an idea going back more than two decades [31] and suggests the following implementation for the Sikivie axion experiment. The "front-end" of the experiment is the same, *i.e.* there is a tunable cavity for axion-photon conversion. Photons from this cavity are coupled out to a field-free antechamber, also tuned to the same

frequency. An atomic beam is prepared to the desired Rydberg level by optical pumping, which then traverses the antechamber. Here, however, the spacing of the transition levels must be adjusted to match the frequency of the cavity: this may be accomplished through the Stark effect, by applying a small DC voltage in a parallel-plate configuration. It is here that the Rydberg atoms absorb the microwave photons.

Upon exiting the chamber, the atomic beam is now a mixture of two states, with most of the atoms in the prepared state, and very few atoms promoted to the higher Rydberg level. Detection of only those atoms which have absorbed the microwave photon of the correct frequency is accomplished by selective field ionization. After exiting the chamber, the beam passes through a uniform prescribed electric field, perpendicular to its velocity. The combined Coulomb plus linear potential has a saddle point, or potential barrier, whose height is set precisely (through the applied electric field) such that the electrons promoted to the upper level are unbound, *i.e.* simply fall out of the atom, whereas those in the initial state remain bound. Just as in a photomultiplier tube, the free electron is then accelerated and detected. In practice, one may discriminate between energy levels differing by only a few 10's of MHz.

There are several challenges in implementation. At the most fundamental level, the quantum mechanical interaction of the Rydberg states with the cavity ("Cavity QED") is non-trivial. Addditionally, there are coherent interactions of Rydberg atoms in the cavity. At the more practical level, the "turn-on" of fields seen by the atoms must be adiabatic so as not to project the many Rydberg states onto several Stark states. Similarly, the Rydberg states are only weakly bound and slight perturbations may induce non-selective ionization. Lastly, the energy (frequency) resolution with which an axion signal may be resolved is limited by the transit time of the atoms through the cavity, and would seem marginal for the virialized component. Sensitivity to fine-structure does not seem possible.

An experiment utilizing Rydberg atom single-quantum detection in Kyoto is well along in commissioning ('CARRACK' for Cosmic Axion Research with Rydberg Atoms in a Resonant Cavity in Kyoto).[32] A sketch of the apparatus is shown in Figure 14. The microwave resonator is a single copper cavity (4.5 cm radius, 72.5 cm long) which fits inside a superconducting solenoid (15 cm diameter, 50 cm long, 7 T peak field). Power from the conversion cavity is coupled to a niobium superconducting cavity just above it, where the magnetic field is canceled by a bucking coil. The frequency of both cavities are made to track by means of 6 mm sapphire rods inserted axially into them. The cavities are cooled to < 15 mK by means of a dilution refrigerator.

A beam of rubidium atoms is accelerated, neutralized and directed verti-

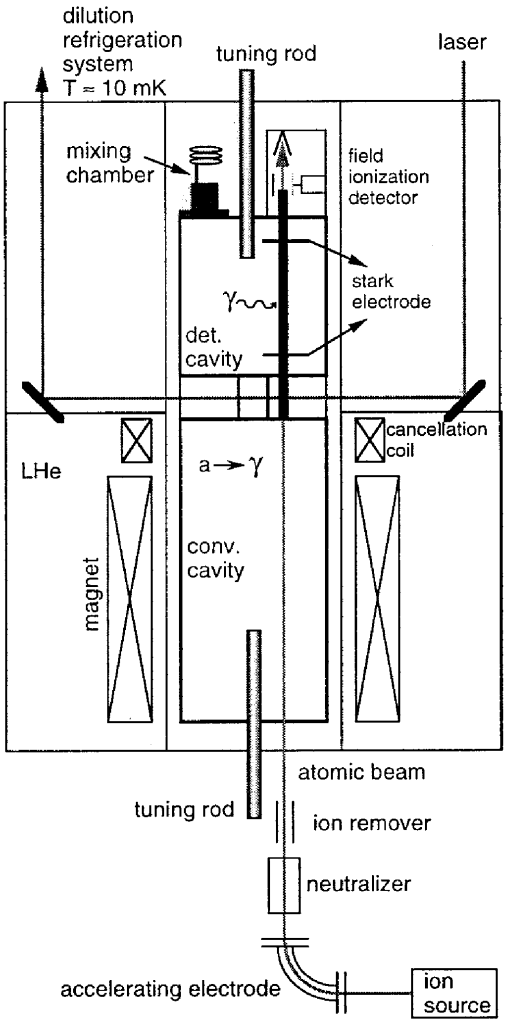

Figure 14: Schematic diagram of the experimental system to search for axions with Rydberg atoms in cooled resonant cavities.

cally through the detection cavity. Just before entering the detection cavity, the atoms are excited to a Rydberg state with principal quantum number near 160, by triple optical excitation with three colinear diode laser beams. In the detection cavity, the Rydberg atoms are then Stark-tuned so an E1 $np \rightarrow (n+2)s$ transition is matched to the cavity frequency. After exiting, the Rydberg atoms are selectively ionized by an electric field (around 0.5 V/cm) and the liberated electron is detected and amplified by an electron multiplier ("Channeltron").

Studies have been performed to confirm that the experiment is sensitive to single blackbody photons in the < 15 mK range. These include verifying the temperature dependence, and the number and velocity of the Rydberg atoms.[33] Several percent of mass range around 2.4 GHz ($\sim 10\mu eV$) has been swept out, but candidate peaks have not been eliminated yet, nor have potential systematic backgrounds been rejected.

4 Conclusion

Our experiment has already demonstrated that Sikivie-type axion detectors can reach the sensitivity to detect galactic halo axions with plausible coupling to photons. Multiple cavity arrays will extend the mass coverage while SQUID based amplifiers will increase the sensitivity and allow us to search for DFSZ axions comprising only a fraction of the halo. The Rydberg atom single-quantum detector could improve the power sensitivity by yet another order of magnitude.

Acknowledgments

The collaboration associated with the current dark-matter axion experiment is very much indebted to Prof. Adrian Melissinos, not only for his technical contributions and physical insight, but more importantly for his enthusiasm and sense of excitement that he brought to the field. We especially acknowledge his role in helping catalyze the present experiment, by his organization of the Workshop on Cosmic Axions at BNL, April 13-14, 1989.[34]

This work was performed under the auspices of the U.S. Department of Energy by the University of California, Lawrence Livermore National Laboratory under Contract No. W-7405-Eng-48.

References

1. R. Peccei and H. Quinn, *Phys. Rev. Lett.* **38**, 1440 (1977).
2. S. Weinberg, *Phys. Rev. Lett.* **40**, 223 (1978); F. Wilczek, *ibid.* 279 (1978).

3. J. Preskill, M. Wise, and F. Wilczek, *Phys. Lett.* **120**, 127 (1983); L. Abbott and P. Sikivie *ibid.*, 133; M. Dine and W. Fischler. *ibid.*, 137; M.S. Turner, *Phys. Rev.* D **33**, 889 (1986).
4. G.G. Raffelt, *Stars as Laboratories for Fundamental Physics.* University of Chicago Press, Chicago (1996).
5. A.D. Linde, *Phys. Lett.* B **201**, 437 (1988).
6. J.E. Kim, *Phys. Rev. Lett.* **43**, 103 (1979); M.A. Shifman. A.I. Vainshtein, and V.I. Zakharov, *Nucl. Phys.* **166**, 493 (1980).
7. M. Dine, W. Fischler, and M. Srednicki, *Phys. Lett.* **104**, 199 (1981); A.R. Zhitnitsky, *Sov. J. Nucl. Phys.* **31,** 260 (1980).
8. M.S. Turner *Phys. Rev.* D **33**, 889 (1986).
9. P. Sikivie, *Phys. Rev. Lett.* **51**, 1415 (1983).
10. L. Krauss *et al.*, *Phys. Rev. Lett.* **55**, 1797 (1985).
11. E. I. Gates, G. Gyuk, and M.S. Turner, *Astrophys. J.* **449**, 123 (1995).
12. L.J. Rosenberg and K. van Bibber, *Phys. Rep.* to be published.
13. S. DePanfilis *et al.*, *Phys. Rev. Lett.* **59**, 839 (1987), W. Wuensch *et al.*. *Phys. Rev.* D **32**, 2988 (1980).
14. C. Hagmann *et al.*, *Phys. Rev.* D **42**, 1297 (1980).
15. B. Moskowitz and J. Rogers, *Nucl. Inst. and Meth.* **A264**, 445 (1988).
16. C. Hagmann *et al.*, *Rev. Sci. Instr.* **61**, 1076 (1990).
17. Wang NMR Inc., 550 N. Canyons Parkway, Livermore, CA 94550.
18. E. Daw and R.F. Bradley, *J. Appl. Phys.* **82**, 1925 (1997).
19. Stanford Research Systems,1290-D Reamwood Ave., Sunnyvale, CA 94089.
20. M.S. Turner, *Phys. Rev.* D **42**, 3572 (1990).
21. P. Sikivie and J. Ipser, *Phys. Lett.* B **291**, 288 (1992).
22. P. Sikivie *et al.*, *Phys. Rev. Lett.* **75**, 2911 (1995).
23. National Instruments,11500 N. Mopac Expwy., Austin, TX 78759.
24. C. Hagmann *et al.*, *Phys. Rev. Lett.* **80**, 2043 (1998).
25. C.D. Tesche and J. Clarke, *J. Low Temp. Phys.* **27**, 301 (1977).
26. M. Mück, M.-O. André, J. Clarke, J. Gail, and C. Heiden., *Appl. Phys. Lett.* **72**, 2885 (1998).
27. M. Mück, M.-O. André, J. Clarke, J. Gail, and C. Heiden., Submitted to *App. Phys. Lett.*
28. J. Clarke, *Proc. of the NATO ASI on SQUID Sensors: Fundamentals, Fabrication and Applications*, Kluwer Academic Publishers, H. Weinstock ed. (1996).
29. M. Mück, M.-O. André, J. Clarke, J. Gail, and C. Heiden., *Appl. Phys. Lett.* **75**, 698 (1999).
30. T.F. Gallagher, *Rydberg Atoms*, Cambridge University Press, Cambridge

(1994).
31. D. Kleppner and T.W. Lucas, *Bull. Am. Phys. Soc.* **21**, 200 (1976).
32. I. Ogawa *et al., Proc. of the 2nd RESCEU International Symposium on "Dark Matter in the Universe and its Direct Detection,"* Universal Academy Press, Inc. (Tokyo), M. Minowa ed. (1997).
33. S. Matsuki, private communication (1998).
34. *Proc. of the Workshop on Cosmic Axions,* World Scientific (Singapore), C. Jones and A. Melissinos ed. (1990).